STM JOURNALS

Research & Reviews: Journal of Physics
ISSN: 2278-2265 (Online), ISSN: 2347-9973 (Print)
Volume 6, Issue 1
www.stmjournals.com

Research on Laser Hardened Bead Geometry in Laser Hardening Parameters of ASTM Grade3 Pure Titanium

Duradundi Sawant Badkar*
Department of Mechanical Engineering, Shri Balasaheb Mane Shikshan Prasarak Mandal Ambap's, Ashokrao Mane Group of Institutions, Vathar Tarf Vadgaon, Kolhapur, Maharashtra, India

Abstract

In the presented study, the laser transformation hardening of commercially pure titanium sheet material of thickness being 1.6 mm is investigated using CW (continuous wave) 1.6 kW solid state Nd:YAG laser. Commercially pure titanium has widespread application in various fields of industries including the medical, nuclear, automobile and aerospace. A full factorial design (FFD) with response surface methodology (RSM) is employed to establish, optimize and to investigate the relationships of three laser transformation hardening process parameters such as laser power, scanning speed, and focused position on laser hardened bead profile parameters such as hardened bead width, hardened depth, heat input. RSM is used to develop pseudo-closed-form models from the computational parametric studies. Effects of laser process parameters: laser power, scanning speed and focal point position on laser hardened bead geometries such as hardened bead width, hardened depth and heat input were carried out using RSM. Results indicate that the scanning speed and laser power have the significant effect as compared to the focal point position on the laser hardening process parameters. The scanning speed has a positive effect on all responses while the laser power has a positive effect particularly on hardened bead width and as compared to hardened depth and heat input. The optimum laser hardening conditions are identified sequentially to minimise hardened depth, heat input, and maximum hardened bead width. The validation results demonstrate that the developed models are accurate with low percentages of error (less than 7.409%).

Keywords: *Laser transformation hardening; response surface methodology; full factorial design; analysis of variance; bead geometry*

****Author for Correspondence*** E-mail: dsbadkar@gmail.com

INTRODUCTION

The basic laser transformation hardening of titanium and its alloys consists of two major stages: (i). Beta phase formation, in which the material is heated to/above the beta transus temperature, i.e., β-transus (888°C or 1621°F), in order to form the material with 100% beta phase (but below the melting point) and (ii). "Self-quenching" or cooling down, where, the β-phase is transformed into harder acicular (plate-like) α martensite (transformed β) or maintain β phase (beta) to room temperature. The β-transus is defined as the lowest equilibrium temperature at which the material is 100% beta or alpha, which does not exist. It has been confirmed that the β-transus is critical in deformation processing and in heat treatment processes. A correct heat treatment involves the heating stage be long enough for the β-phase formation to complete and permit the alloying elements such as manganese, carbon, oxygen and nitrogen to stabilize it and dissolve iron, molybdenum, copper, nickel, vanadium and silicon into the matrix. Self-quenching should be quick enough so as to control the normal breaking down of β-phase into the initial α or α+ β phases and produce martensite instead [1].

The literature survey reveals that many authors have published their research work related to only laser welding process types and steel material, with full factorial design, Box–Behnken design, Plackett-Burman design, and central composite design using response surface methodology. D.S. Badkar *et al.* studied the effects of laser transformation hardening variables on the heat input and hardened-bead geometry quality of commercially pure titanium using Box–Behnken design with response

surface methodology [1]. From literature survey, it has been observed that papers specifically related to an optimization and effects of laser transformation hardening of commercially pure titanium have been not published, but in this research paper the authors absolutely focused their research work on an optimization and effects of laser transformation hardening parameters of titanium using full factorial design with response surface methodology. In this research paper an attempt has been made to establish an empirical relationship between the laser hardening process parameters: laser power, scanning speed, focused position and bead profile parameters such as hardened bead width, hardened depth, and, heat input using response surface methodology by full factorial design matrix. Authors specifically studied and showed the effects of laser hardening parameters and heat input on hardened bead geometry.

U. Reisgen *et al.* in their research work, numerical and graphical optimisation techniques of the CO_2 laser beam welding of dual phase (DP600)/transformation induced plasticity (TRIP700) steel sheets were carried out using response surface methodology (RSM) based on Box–Behnken design [2]. Kamal Pal et al. in their article developed the modelling and optimisation of deposition efficiency in highly non-linear pulsed metal inert gas welding. They performed the design of experiments using central composite design matrix and developed the model by response surface methodology [3]. G. Padmanaban *et al.* developed an empirical relationship to between the tensile strength and pulsed current gas tungsten arc welded AZ31B magnesium alloy welding process parameters [4]. Sanjay Kumar et al. conducted the experiments on square butt joint plate of 5083 H111 aluminium alloy using full the factorial design of experiments and established the mathematical models for depth of penetration and convexity formation were established by using multiple nonlinear regression analytical models and are checked for their adequacy [5]. Xiao Yun Zhang et al. used the response surface methodology (RSM) to study the influence of laser welding parameters on weld seam quality [6]. R. Palanivel *et al.* established a systematic approach to develop the mathematical model for predicting the ultimate tensile strength, yield strength and percentage of elongation of AA6351 aluminum alloy which is extensively used in automobile industries, aircraft engines and defense industries by integrating friction stir welding process parameters such as tool rotational speed, welding speed, and axial force [7]. Ali Khorram et al. employed Response Surface Methodology (RSM) to establish the design of experiments and to optimize the bead geometry of CO_2 Laser Welding of Ti 6Al 4V [8]. S Rajakumar et al. developed an empirical relationship between the friction-stir-welding process and tool input variables to achieve a maximum tensile strength of AA7075–T6 aluminium alloy using response surface methodology [9]. A.Vairis and M. Petousiset et al. applied the parametric design of the experiments the fractional factorial method to assess the effect of a number of factors on the impact strength of linear friction welding of Ti6Al4V joints [10].

K.Y. Benyounis, developed an empirical relationship between the welding process parameters and the output variables of the welded joint so as to establish the welding parameters that lead to the desired weld quality using the design of experiment (DoE) [11]. Ali Alidoosti *et al.* based on full factorial design the Electrical discharge machining characteristics of nickel–titanium shape memory alloy has been investigated [12]. S.L. Chen *et al.* used Analysis of Variance (ANOVA) methodology to find the optimal laser process parameters and to evaluate quantitatively the quality characteristics of laser transformation hardening of SNCM 439 steel by a long-pulsed Nd-YAG laser beam. They obtained a significant improvement in the quality of laser transformation hardening by Nd-YAG laser [13]. Ruifeng Li *et al.* investigated the laser surface hardening in the AISI 1045 steel using two kinds of industrial lasers such as high-power diode laser (HPDL) and a CO_2 laser, respectively and studied the effect of process parameters such as beam power, travel speed on structure and case depth of hardened steel [14]. Shuang Liu et al. carried out a systemic study on the HPDDL cladding process by depositing Fe-based powder on ASTM A36 steel base material. The influences of input process parameters: laser power, powder feeding rate, carrier-gas

flow rate, and stand-off distance on the output responses such as powder catchment efficiency, height of clad and width of clad were analyzed. The experiments were conducted by central composite design matrix and a quadratic regression models were developed using a response surface methodology (RSM) and tested by the analysis of variance (ANOVA) method, the relationship between the output responses and the processing parameters were analyzed and discussed [15]. Yangyang Zhao *et al*. response surface methodology (RSM) was used to develop models to predict the relationship between the processing parameters: laser power, welding speed, gap and focal position and the laser weld bead profile: weld depth, weld width and surface concave and identify the correct and optimal combination of the laser welding input variables to obtain superior weld joint [16].

In this study, the influence of laser process parameters: laser power, scanning speed and focused position on hardened bead geometry of the commercially pure titanium has been investigated. Response surface methodology is used for experimental design. Twenty-seven experimental laser transformation hardening bead on trials was performed on the commercially pure titanium alloy using a CW 1.62 KW Nd:YAG laser machine. Statistical tools such as the design of experiments, analysis of variance, and regression analysis are used to develop the relationships. The developed empirical relationship can be effectively used to predict the laser transformation hardening of commercially pure titanium at the 95% confidence level. Finally, the Response surface methodology is used to model the laser transformation hardening process.

EXPERIMENTAL DESIGN

DOE techniques allow the engineer to change multiple factors simultaneously; such an approach considerably reduces the number of experiments required and also allows the engineer to investigate interactions and higher order effects. A full-factorial design allows the analysis of effects of main factors, interactions, and, depending on the factor levels, higher order effects. An interaction can be thought of as a new factor which is a combination of two or more factors. Interactions are not intuitive and their effects are hard to predict. Even if a DOE is more efficient than a one-factor-at-a-time approach, the matrix can still be very large and may not be suitable for a variety of reasons including lack of necessary materials, lack of time available on the machine, lack of man-hours, or all of the above. For example, a process with 5 factors evaluated at 2 levels will require 25 =32 experiments for a full-factorial [17–20].

Response surface methodology (RSM) is a tool that was introduced in the early 50's by Box and Wilson (1951) [21]. It is a collection of mathematical and statistical techniques useful for the approximation and optimisation of stochastic models. Applications of RSM can be found in e.g. chemical, engineering and clinical sciences. Response surface methodology (RSM) is an empirical, technique involving the use of design expert software to derive a predictive model similar to regression analysis [22].

A 3-factor, the 3-level design used is suitable for exploring quadratic response surfaces and constructing second-order polynomial models. This quadratic design model is given by a set of points at the midpoint of each edge of a multidimensional cube and a centre point replicate. The nonlinear computer-generated (Statgraphics, Manugistics Inc, Rockville, MD) quadratic model is given as;

$$Y = b_0 + b_1 \times_1 + b_2 \times_2 + b_3 \times + b_{12} \times_1 \times_2 + b_{13} \times_1 \times_3 + b_{23} \times_2 \times_3 + b_{11} \times_{12} + b_{22} \times_2^2 + b_{33} \times_3^2$$

Where, Y is the measured response associated with each factor level combination; b_0 is an intercept; b_1 to b_{33} are the regression coefficients; and X_1, X_2, and X_3 are the independent variables [23]. The dependent and independent variables selected are shown in Table 2. These high, medium, and low levels were selected from the preliminary experimentation.

EXPERIMENTAL METHODOLOGY

Full Factorial Designs (FFD) are response surface designs specially made to require only 3 levels, coded as -1, 0, and +1. The experiments are conducted based on the three factors, three levels full factorial design of

experimental methodology [24]. As per this technique, total numbers of experiments considered for conducting the experiments are 3^3=27 as there are three input process parameters each at three levels. Therefore, a total of 27 experiments were carried out for each configuration. Table 1 shows the chemical composition of commercially pure titanium of ASTM Grade3 used for the experimental investigation. The selected values of the process parameters along with their units and notations are given in Table 2.

Experiments are carried out using A CW (continuous wave) 2 kW, with radiation wavelength λ= 1.06 μm Nd:YAG laser source from GSI Lumonics as shown in Figures 1 and 2 shows a photograph of the corresponding experimental setup. A continuous wave Gaussian spherical beam configuration was used throughout the experimental work. A 120 mm focal optic was used with varying beam spot size depending on a defocusing distance to obtain a wide scan area. Pure argon gas is used as shielding medium and is supplied at the constant flow rate of 10 litres/min.

Transverse section specimens were cut from laser hardened-bead on trials of commercially pure titanium sheet and mounted using Araldite. Standard metallographic was made for each transverse sectioned specimen. An optical microscope used for measurement was a portable video microscope, LM525 having image processing computer controlled software based on LINUX OS 9.3 with digital micrometres attached to it with an accuracy of 0.001 mm, which allowed to measure directional movement in x-axes and y-axes.

Table 1: *Chemical Composition of Commercially Pure Titanium.*

Element	Ti	C	Fe	Mo	V	Zr	Cu	O	N	Al
% by Weight	Bal.	0.011	0.15	0.003	0.029	0.0039	0.14	0.1	0.003	1.1

Table 2: *Process Variables and Experimental Design Levels Used.*

Variables			-1	0	1
Laser power, (Watts)	LP	X1	750	1000	1250
Scanning speed, (mm/min)	SS	X2	1000	2000	3000
Focused position, (mm)	FP	X3	-30	-20	-10

Fig. 1: *Solid State Nd:YAG Laser Source at WRI Used for Experimental Work [25].*

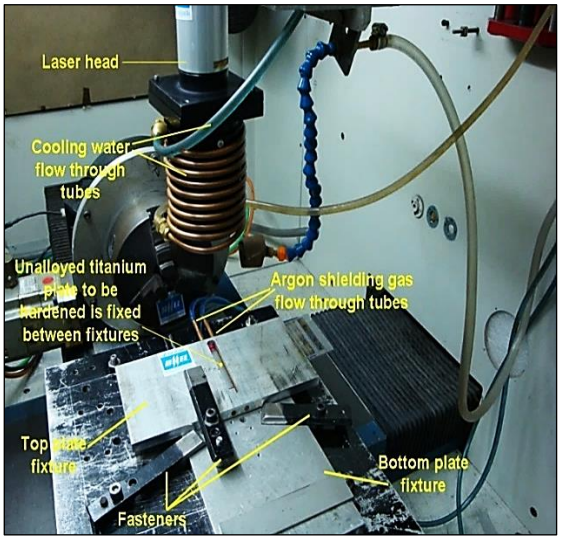

Fig. 2: *Experimental Set-up Showing the Laser Beam Head and Shielding Arrangements in the Working Chamber [25].*

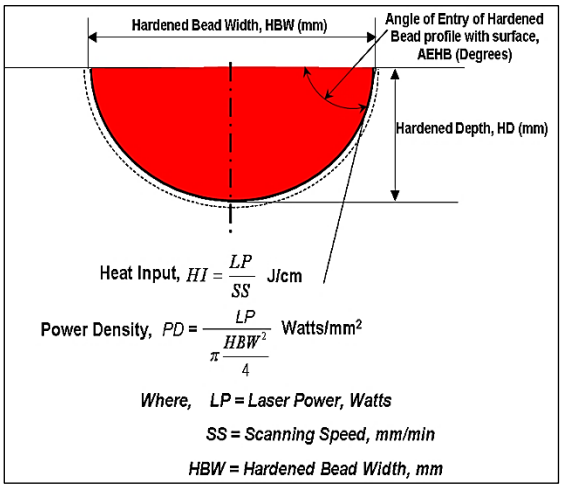

Fig. 3: *The Schematic Diagram of Laser Hardened-Bead Profile Geometry with Experimental Measurable Responses.*

Figure 3 shows the schematic diagram of laser hardened-bead profile geometry with experimental measurable responses. The measured laser hardened bead profile parameters 'responses' were recorded. Table 3 demonstrates the 3^3 full factorial design layout matrix with code independent variables. The serial No of experiments with run order and the measured responses are recorded.

RESULTS AND DISCUSSIONS

The results of the laser hardened-bead profile were measured according to the design matrix with coded independent process variables as shown in Table 3 and are recorded.

Analysis of Variance (ANOVA) for Response Surface Full Model

The adequacy of the developed models was tested using the Analysis of Variance (ANOVA) Technique and the results of the linear and quadratic order response surface models fitting in the form of analysis of variance (ANOVA) are given in Tables 4–6.

The ANOVA Tables 4–6 also shows the model terms adequacy measures R^2, adjusted R^2, predicted R^2, Std. Dev, Mean, C.V and PRESS. In this case, all the values of coefficient of determination R^2 are nearly equal to 1. Clearly, we must have $0 \leq R^2 \leq 1$, with larger values being more desirable. In all the ANOVA Tables, the entire adequacy measures are closer to 1, which is in reasonable agreement and indicate adequacy of models. The adequate precision is greater than 4 in all cases and is desirable. An adequate precision ratio above 4 indicates adequate model discrimination. At the same time, relatively lower values of the coefficient of variation, C.V., from the Tables 4–8 indicates improved precision and reliability of the conducted experiments. Small values of PRESS are desirable. In all the cases the values of PRESS are considerably small [24].

Table 3: *3^3 Full Factorial Design Layout Matrix with Code Independent Variables.*

Exp. No	X_1	X_2	X_3	X_1^2	X_2^2	X_3^2	X_1X_2	X_2X_3	X_1X_3	$X_1X_2X_3$
	LP	SS	FP	LP^2	SS^2	FP^2	LPxSS	SSxFP	LPxFP	LPxSSxFP
1	-1	-1	-1	1	1	1	1	1	1	-1
2	0	-1	-1	0	1	1	0	1	0	0
3	1	-1	-1	1	1	1	-1	1	-1	1
4	-1	0	-1	1	0	1	0	0	1	0
5	0	0	-1	0	0	1	0	0	0	0
6	1	0	-1	1	0	1	0	0	-1	0
7	-1	1	-1	1	1	1	-1	-1	1	1
8	0	1	-1	0	1	1	0	-1	0	0
9	1	1	-1	1	1	1	1	-1	-1	-1
10	-1	-1	0	1	1	0	1	0	0	0
11	0	-1	0	0	1	0	0	0	0	0
12	1	-1	0	1	1	0	-1	0	0	0
13	-1	0	0	1	0	0	0	0	0	0
14	0	0	0	0	0	0	0	0	0	0
15	1	0	0	1	0	0	0	0	0	0
16	-1	1	0	1	1	0	-1	0	0	0
17	0	1	0	0	1	0	0	0	0	0
18	1	1	0	1	1	0	1	0	0	0
19	-1	-1	1	1	1	1	1	-1	-1	1
20	0	-1	1	0	1	1	0	-1	0	0
21	1	-1	1	1	1	1	-1	-1	1	-1
22	-1	0	1	1	0	1	0	0	-1	0
23	0	0	1	0	0	1	0	0	0	0
24	1	0	1	1	0	1	0	0	1	0
25	-1	1	1	1	1	1	-1	1	-1	-1
26	0	1	1	0	1	1	0	1	0	0
27	1	1	1	1	1	1	1	1	1	1

The values of "Probability > F" in Tables 4–6 for all models are less than 0.0500 indicate that all models are significant. In all cases, the "Residuals" values are very small related to the sum of squares of models which implies the R-Squared value nearer to 1. Very small values of "Residuals" are desired and it is good.

Table 4: *ANOVA Table for Heat Input (Reduced Quadratic Model).*

Source	**Sum of Squares**	**df**	**Mean Square**	**F Value**	**p-value Prob > F**	
Model	961250	4	240313	2114.75	< 0.0001	Significant
LP	151250	1	151250	1331	< 0.0001	
SS	720000	1	720000	6336	< 0.0001	
LP x SS	30000	1	30000	264	< 0.0001	
SS^2	60000	1	60000	528	< 0.0001	
Residual	2500	22	113.636			
Corrected Total	963750	26				
Std. Dev.	10.660	R-Squared			0.9974	
Mean	366.67	Adjusted R-Squared			0.9969	
C.V. %	2.9073	Predicted R-Squared			0.9960	
PRESS	3881.5	Adequate Precision			127.16	

Table 5: *ANOVA Table for Hardened Bead Width (Reduced Quadratic Model).*

Source	**Sum of Squares**	**df**	**Mean Square**	**F Value**	**p-value Prob > F**	
Model	3.1435	4	0.7859	110.611	< 0.0001	significant
LP	1.6362	1	1.6362	230.3	< 0.0001	
SS	1.0844	1	1.0844	152.625	< 0.0001	
FP	0.2298	1	0.2298	32.3501	< 0.0001	
LP x SS	0.193	1	0.193	27.1703	< 0.0001	
Residual	0.1563	22	0.0071			
Corrected Total	3.2998	26				
Std. Dev.	0.0843	R-Squared			0.9526	
Mean	2.2311	Adjusted R-Squared			0.944	
C.V. %	3.7779	Predicted R-Squared			0.9264	
PRESS	0.2428	Adequate Precision			36.388	

Table 6: *ANOVA Table for Hardened Depth (Reduced Quadratic Model).*

Source	**Sum of Squares**	**df**	**Mean Square**	**F Value**	**p-value Prob > F**	
Model	2.0970	6	0.3495	88.8858	< 0.0001	significant
LP	0.6494	1	0.6494	165.16	< 0.0001	
SS	1.2236	1	1.2236	311.177	< 0.0001	
FP	0.0471	1	0.0471	11.9847	0.0025	
LP x SS	0.1184	1	0.1184	30.1127	< 0.0001	
LP^2	0.0204	1	0.0204	5.18246	0.034	
SS^2	0.0381	1	0.0381	9.69814	0.0055	
Residual	0.0786	20	0.0039			
Corrected Total	2.1757	26				
Std. Dev.	0.0627	R-Squared			0.9639	
Mean	0.6414	Adj R-Squared			0.953	
C.V. %	9.7769	Predicted R-Squared			0.9355	
PRESS	0.1404	Adequate Precision			31.435	

Initially, the analysis of variance from the Table 4 indicates that for the HI model, the main effect of the laser power (LP), scanning speed (SS), two-level interaction of laser power and scanning speed (LP×SS) and the second order effect of scanning speed (SS) are the most significant model terms associated with heat input.

Secondly, for the hardened bead width (HBW) model, the analysis of variance (ANOVA) Table 5 denoted that there is a quadratic relationship between the main effects of the three process parameters. Also, in the case of HBW model, from the Table 5, the main effect of LP, SS, FP, and interaction effect of LP with SS have the significant effect. However, the main effect of SS and the main effect LP are the most significant factors associated with the hardened bead width as compared to focused position.

Thirdly, for the hardened depth (HD) model, from the Table 6 it is observed that the main effect of LP, SS, FP, interaction effect of laser power with focused position (LP×FP), second order effect of laser power (LP^2), and second order effect of scanning effect (SS^2) have significant effects on the HD model. Though, the main effect of SS and the main effect are the most significant factors associated with the HD, in comparison with the main effect of FP.

All above consideration indicates an excellent adequacy of the response surface multiple regression models. Each observed value is compared with the predicted value for all the models are shown by the scatter diagrams from the Figures 4–6 respectively. The final mathematical models in terms of coded factors as determined by design expert software are given below:

$$\text{Heat Input (HI)} = 300+91.667LP - 200\,SS - 50\,LPxSS + 100\,SS^2 \quad (1)$$

$$\text{Hardened Bead Width (HBW)} = 2.2311+0.3015LP - 0.2454SS - 0.1130FP - 0.1268LPxSS \quad (2)$$

$$\text{Hardened Depth (HD)} = 0.6271+0.1899LP - 0.2607SS+0.0512FP - 0.0993LPxSS - 0.0583LP^2 + 0.0797SS^2 \quad (3)$$

While the following final empirical models in terms of actual factors:

$$\text{Heat Input (HI)} = 333.333+0.76667LP - 0.40SS - 0.0002LP \times SS + 0.0001SS^2 \quad (4)$$

$$\text{Hardened Bead Width (HBW)} = 0.2753 + 0.00222LP + 0.00026SS - 0.0113FP - (5E-07)\,LP \times SS \quad (5)$$

$$\text{Hardened Depth (HD)} = -0.9171 + 0.0034LP - 0.0002SS + 0.0051FP - (4E-07)\,LPxSS - (9E-07)\,LP^2 + (8E-08)SS^2 \quad (6)$$

Validation of the Models

Figures 4–6 show the relationship between the actual and predicted values of the heat input, hardened bead width, hardened depth respectively. These Figures 4–6 indicate that the developed models are adequate because the residuals in a prediction of each response are minimum since the residuals tend to be close to the diagonal line. Furthermore, to verify the adequacy of the developed models, six confirmation experiments were carried out using new test conditions, but are within the experimental range defined early. Table 7 summarizes the experiments condition, the actual experimental values, the predicted values, error and the percentages of error.

Effect of Process Factors on Hardened Bead Profile Parameters

Heat Input (HI)

The laser heat input (HI) is directly related to the laser power (LP) and scanning speed (SS). It can be calculated directly from the heat input (HI) =LP/SS. The reason of predicting the heat input is to develop a model to include it into optimum step in future work. From the 3D and contours graphs shown in Figures 7 and 8, it is evident that as LP increases and the SS decreases the heat input increases.

Hardened Bead Width (HBW)

Figures 9 and 10 show the effect of process parameter on the hardened bead width (HBW). From the results, it is clear that the two parameters LP and SS are significantly affecting the HBW as compared to FP. From the Figures 9 and 10, it is evident that the HBW linearly increases with increasing LP and decreasing SS. At lower beam travel speed (or scanning speed) the time available for the laser beam to direct contact with the surface is more and hence hardened bead width increases as the scanning speed decreases. Therefore, the heat input increases leading to the more volume of the base material being hardened, consequently, the width

of the hardened zone increases. From Figures 11 and 12 it is clear that as LP increases and FP decreases (i.e. from -10mm to -30mm) the HBW increases. LP should be maintained in such an optimum desired level that increase in LP should not melt the surface but heat the surface only.

From the Figures 13 and 14, it is observed that as the SS decreases and the FP decreases (i.e. from -10mm to -30mm) the hardened bead width increases. The results show also that LP plays very important role in the hardened bead dimensions. An increase in LP results in an increase the HBW, because of increase in the power density. Moreover, increase in the defocused beam, or decrease in focused position (i.e. from -10mm, -20mm, and -30mm respectively) means wide laser beam results in spreading the laser power onto the wide area. Therefore, a wide area of the base metal will be hardened (or heated), leading to an increase in HBW or vise verse.

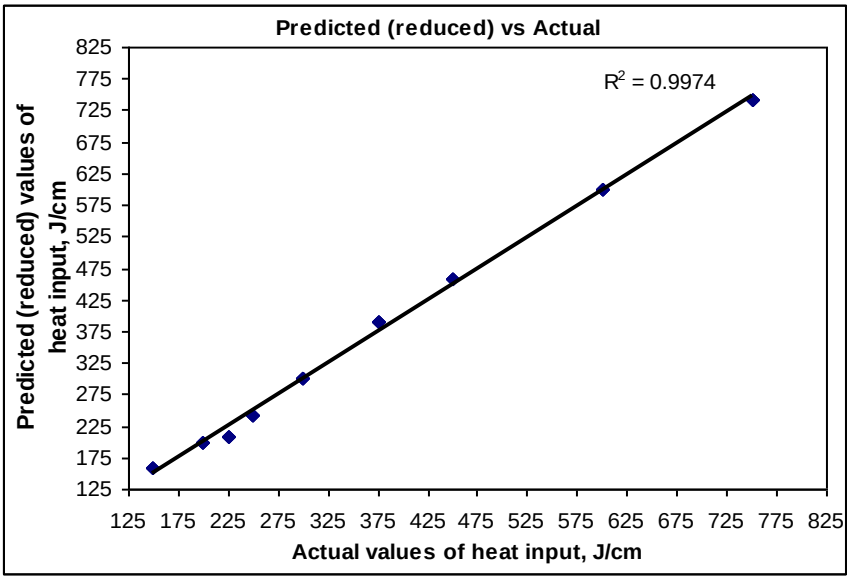

Fig. 4: *Scatter Diagram of Heat Input (HI).*

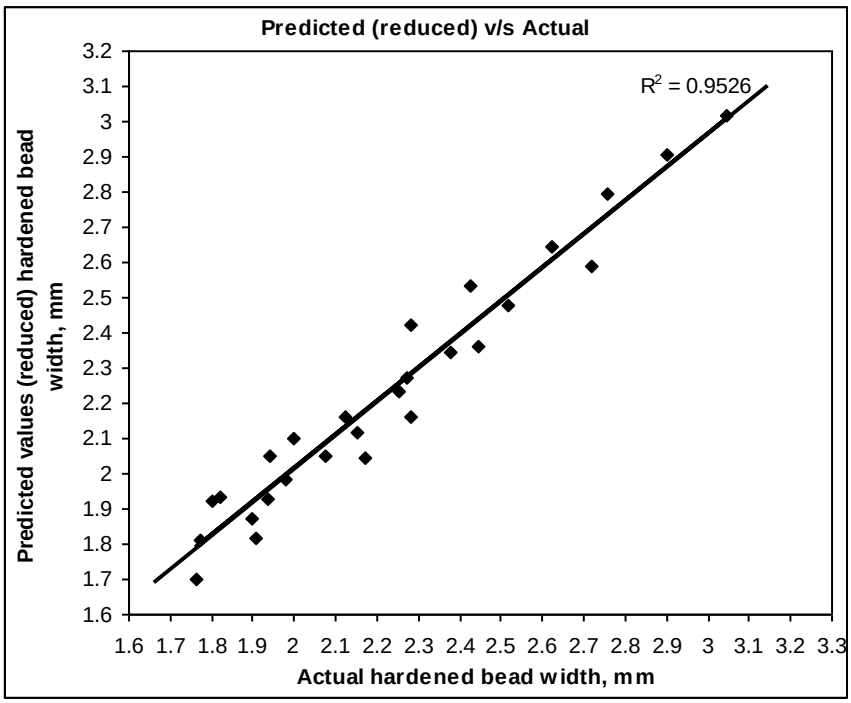

Fig. 5: *Scatter Diagram of Hardened Bead Width (HBW).*

Table 7: *Confirmation of Experiments.*

Exp. No	Process Parameters	Responses	Actual Value	Predicted value	Error	Error %
1	LP=750Watts	HI (J/cm)	150	158.33	-8.33	-5.553
	SS=3000mm/min	HBW (mm)	1.805	1.811	-0.006	-0.332
	FP= -20mm	HD (mm)	0.289	0.297	0.002	0.692
2	LP=750Watts	HI (J/cm)	150	158.33	-8.33	-5.553
	SS=3000mm/min	HBW (mm)	1.767	1.698	0.069	3.904
	FP= -10mm	HD (mm)	0.334	0.348	-0.014	-4.197
3	LP=750Watts	HI (J/cm)	150	158.33	-8.33	-5.553
	SS=3000mm/min	HBW (mm)	1.843	1.924	-0.081	-4.395
	FP= -30mm	HD (mm)	0.243	0.246	-0.003	-1.235
4	LP=750Watts	HI (J/cm)	225	208.33	16.67	7.409
	SS=2000mm/min	HBW (mm)	2.024	2.042	-0.018	-0.889
	FP= -30mm	HD (mm)	0.345	0.328	0.017	4.927
5	LP=750Watts	HI (J/cm)	225	208.33	16.67	7.409
	SS=2000mm/min	HBW (mm)	1.818	1.816	0.002	0.11
	FP= -10mm	HD (mm)	0.477	0.43	0.047	9.853
6	LP=750Watts,	HI (J/cm)	225	208.33	16.67	7.409
	SS=2000mm/min	HBW (mm)	1.921	1.929	-0.008	-0.416
	FP= -20mm	HD (mm)	0.444	0.428	0.016	3.603

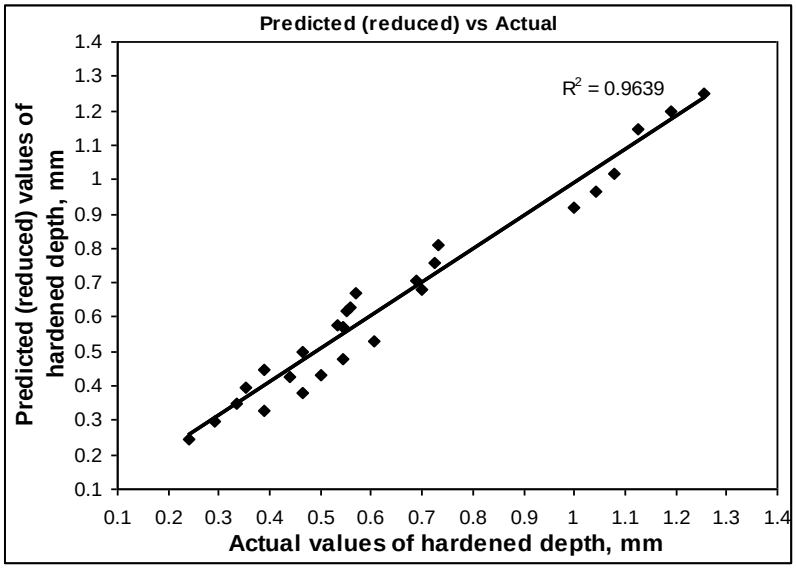

Fig. 6: *Scatter Diagram of Hardened Depth (HD).*

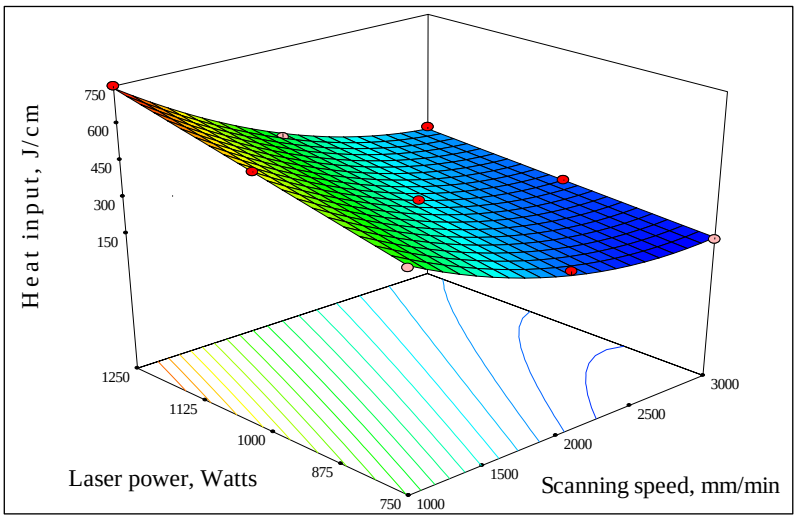

Fig. 7: *3D Graph Shows the Effect of LP and SS on the Heat Input.*

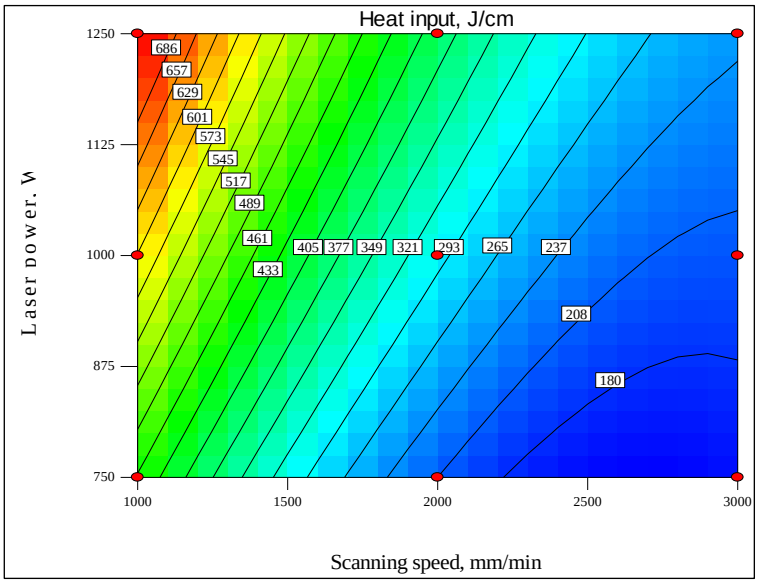

Fig. 8: *Contours Graph Shows the Effect of LP and SS on the Heat Input.*

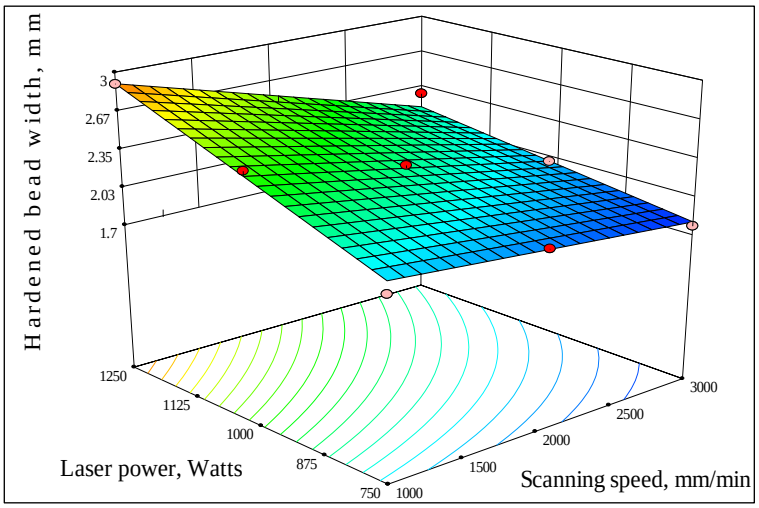

Fig. 9: *3D Graph Shows the Effect of LP and SS on the Hardened Bead Width.*

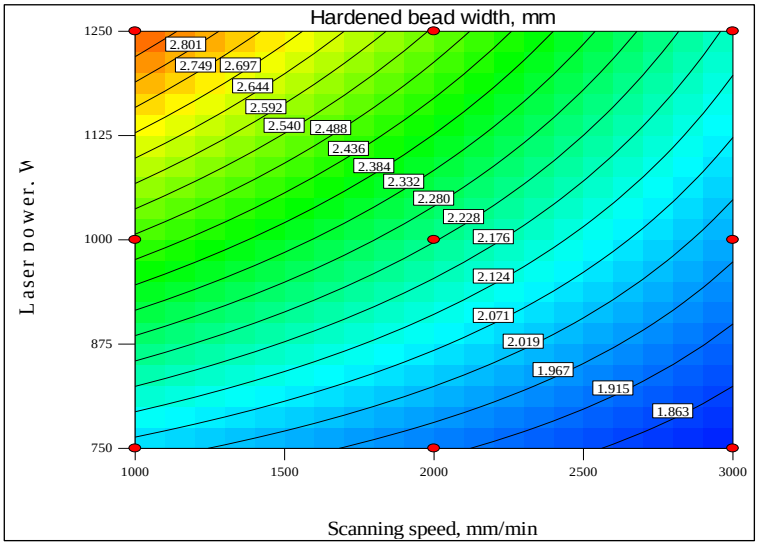

Fig. 10: *Contour Graph Shows the Effect of LP and SS on the Hardened Bead Width.*

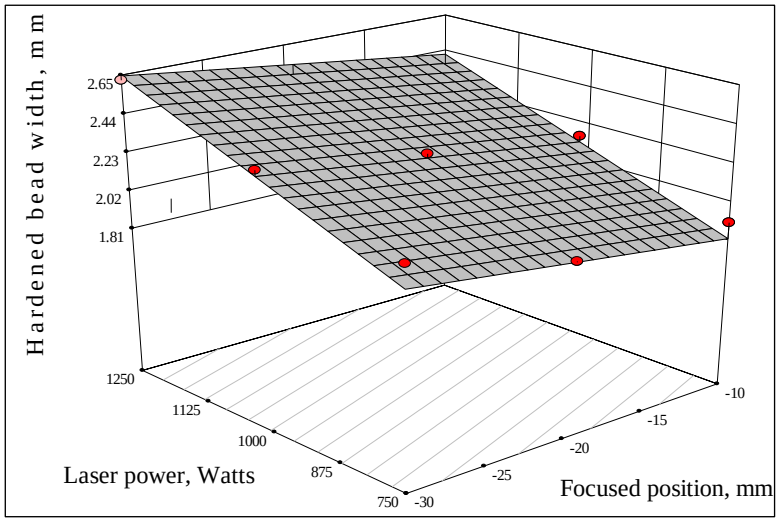

Fig. 11: *3D Graph Shows the Effect of LP and FP on the Hardened Bead Width.*

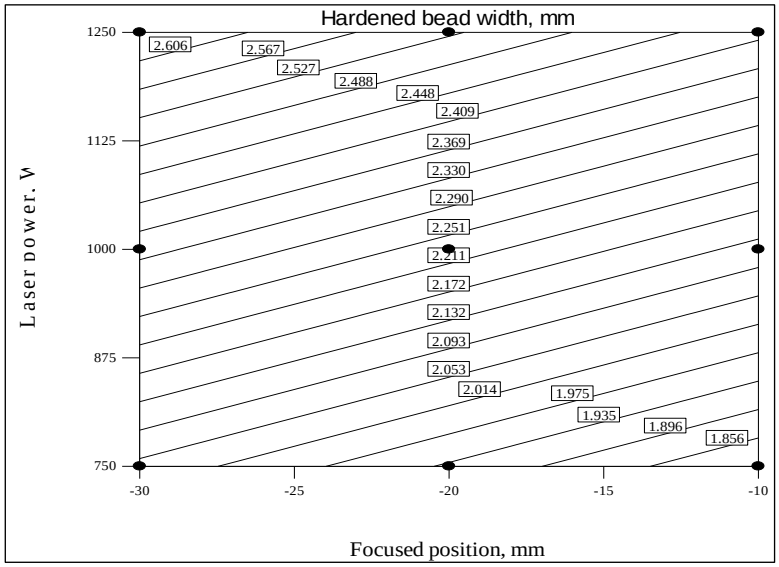

Fig. 12: *Contours Graph Shows the Effect of LP and FP on the Hardened Bead Width.*

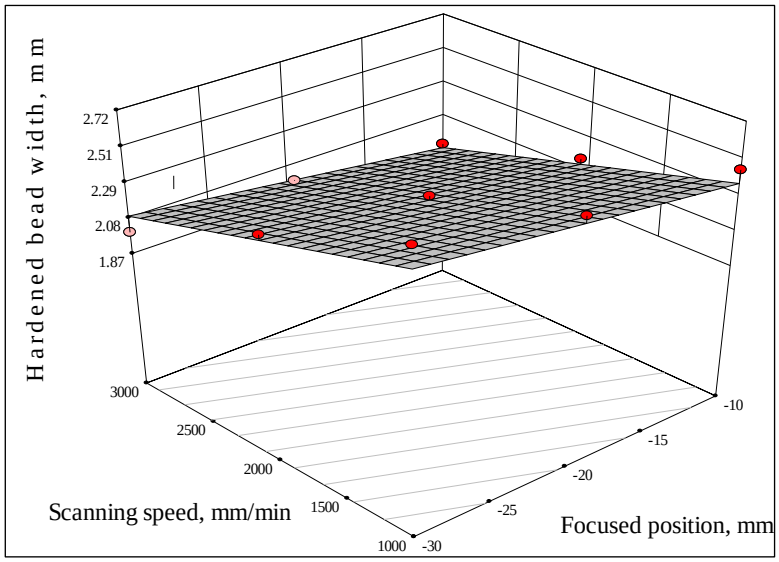

Fig. 13: *3D Graph Shows the Effect of SS and FP on the Hardened Bead Width.*

Hardened Depth (HD)

From the results, it is studied that the parameters those significantly affecting the hardened depth are SS and LP respectively. Effect of focused position on hardened depth is significant but it has less influence as compared to LP and SS. These effects LP and SS are due to following reasons: the increase in LP leads to an increase in the heat input, therefore, more heated fusion metal and consequently more HD will be achieved.

However, the idea is reversed in the case of SS effect, because the SS matches an opposite with HI. From the Figures 15 and 16, it is seen that HD increases as LP increases and SS decreases. From the results obtained it is very important to note that in the case of laser transformation hardening process main aim is to harden the surface with desired optimum depth. As much as possible instead of focusing the beam it is convenient to have defocused beam with negative focal length (i.e. from -10mm, -20mm and -30mm), hence there is no loss of heat energy of laser beam above the focal point, since the laser beam is of converging type, from Figures 17 and 18 it is clear that HD increases with increase in LP and FP (i.e. from -30mm to -10mm). It is also observed from the Figures 19 and 20, it is evident that as SS increases, hardened depth (HD) decreases considerably and as FP increases HD decreases marginally. At lower scanning speed the time available for the laser beam in direct contact with the surface of the base metal is more and hence HD as well as HBW of the hardened surface increases.

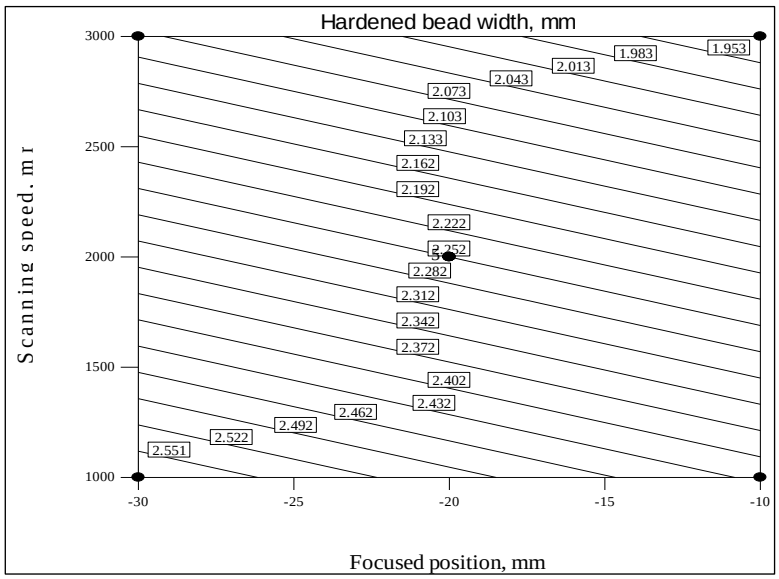

Fig. 14: *Contours Graph Shows the Effect of SS and FP on the Hardened Bead Width.*

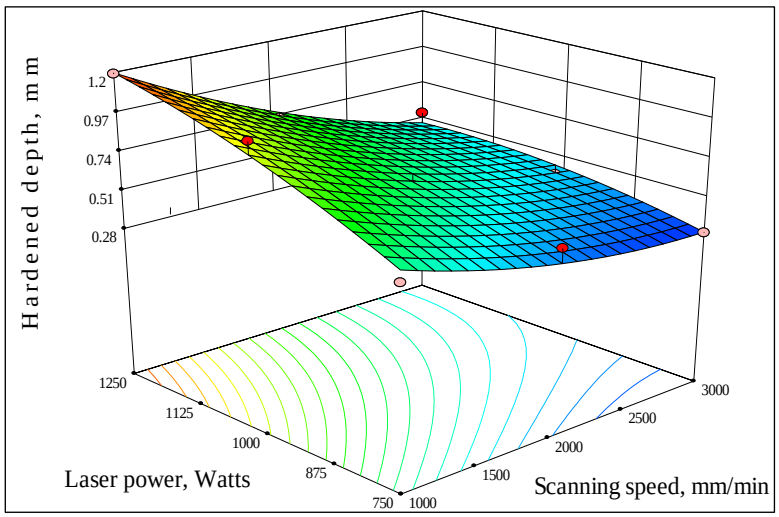

Fig. 15: *3D Graph Shows the Effect of LP and SS on the Hardened Depth.*

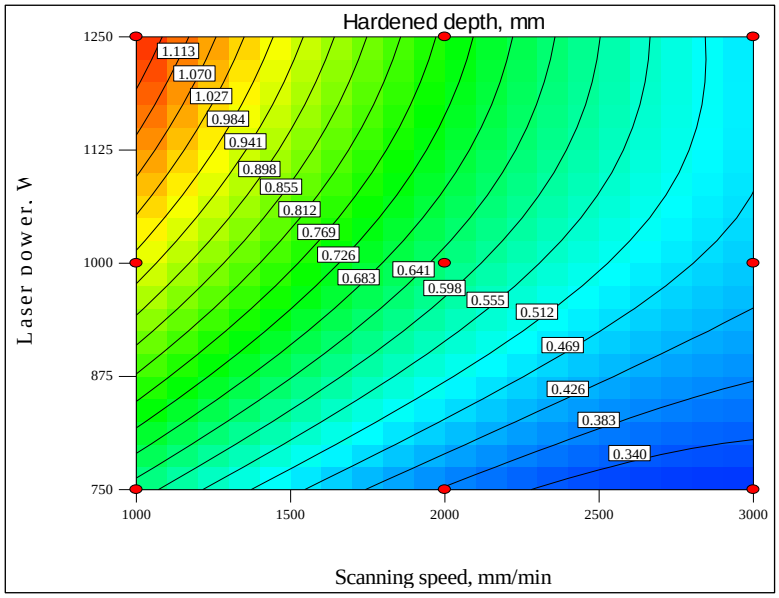

Fig. 16: *Contours Graph Shows the Effect of LP and SS on the Hardened Depth.*

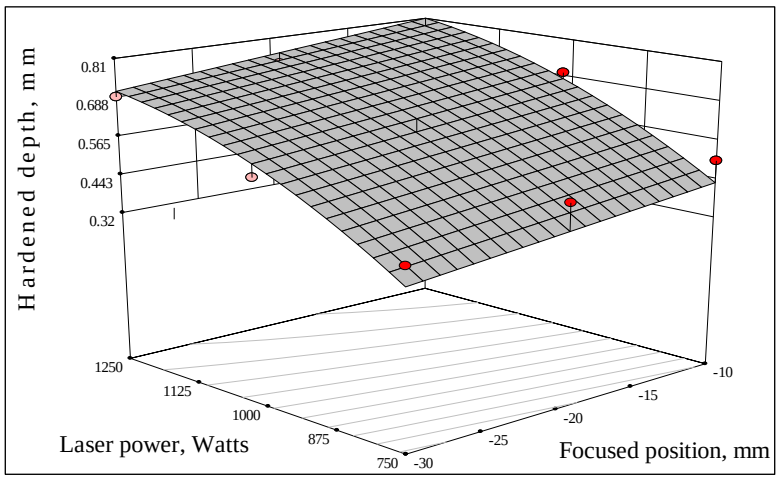

Fig. 17: *3D Graph Shows the Effect of LP and FP on the Hardened Depth.*

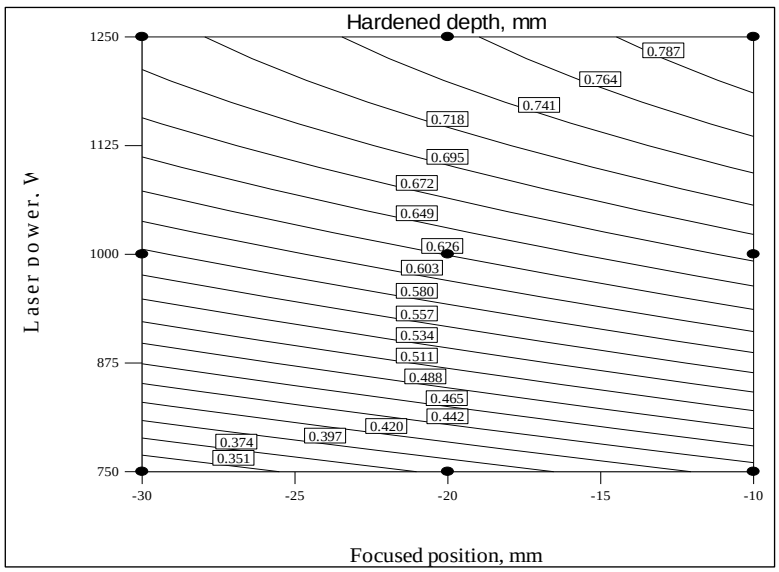

Fig. 18: *Contours Graph Shows the Effect of LP and FP on the Hardened Depth.*

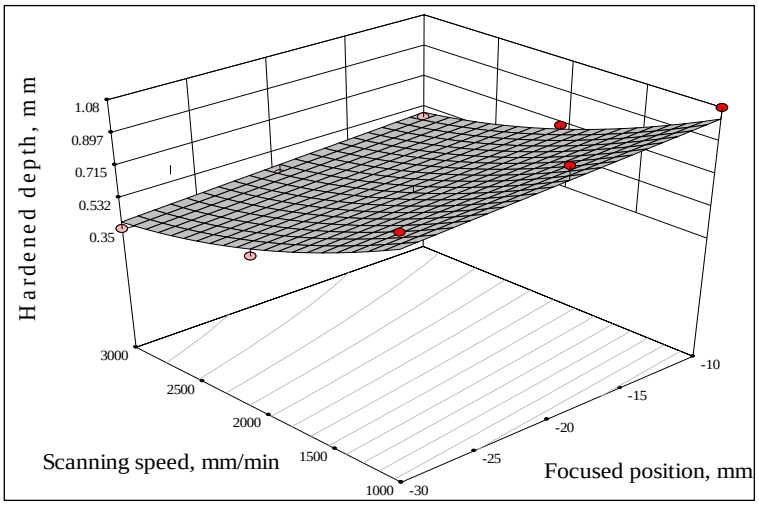

Fig. 19: *3D Graph Shows the Effect of SS and FP on the Hardened Depth.*

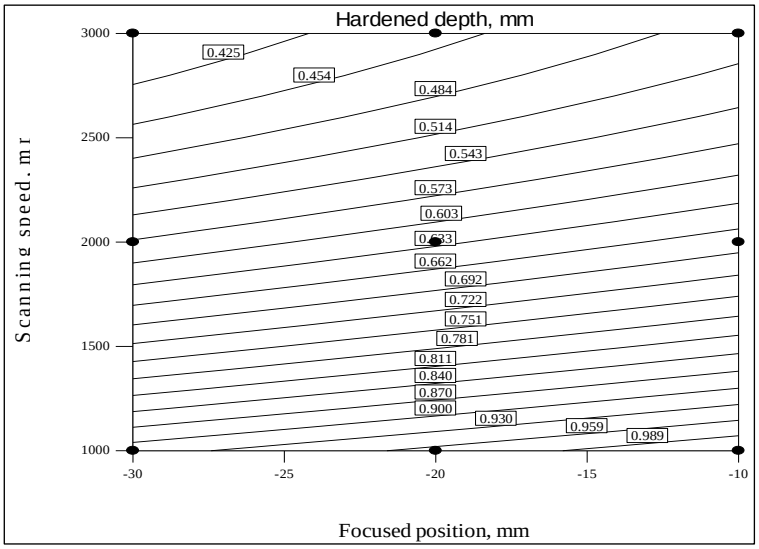

Fig. 20: *Contours Graph Shows the Effect of SS and FP on the Hardened Depth.*

Microstructural Analysis

Figure 21 shows the microstructure of commercially pure (or unalloyed) Titanium, nearer to ASTM Grade 3 chemical composition, consisting of alpha grains and small particles of spheroidal beta, stabilised by the presence of 0.15 % Fe in the alloy. (Etchant: Kroll's reagent -10% HF, 5% HNO_3: 85ml of water, Procedure: Swab 3 to 20 seconds, X200). It is generally observed that the laser hardened surface is smooth, continuous and the heat-affected zone (HAZ) is very narrow. However, the hardened zone and the affected and unaffected base metal are distinct by its structures. Generally, all the microstructures for 27 trials consist of equiaxed α grains and β spheroids stabilised by the presence of 0.15% Fe. From the microstructure, it is observed that laser hardened zone consists of small amount of equiaxed α grains in an acicular α (transformed β) matrix. Formation of acicular martensitic α' (or transformed β), results in the increase in hardness of titanium.

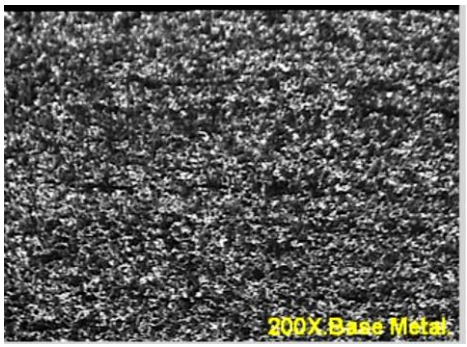

Fig. 21: *Microstructure of Commercially Pure Titanium Base Material [25].*

CONCLUSIONS

The above research work has described the use of design of experiments (DOE) for conducting the experiments. Five models were developed for predicting the heat input (HI), hardened bead width (HBW), hardened depth (HD) of the laser transformation hardened commercially pure titanium by using multiple regression analysis using 33 Full Factorial Design (FFD). The following conclusions were drawn from this investigation within the factors limits considered.

1. Full Factorial Design (FFD) can be employed to develop mathematical models for predicting laser hardened- bead geometry.
2. The desired optimum hardened depth and width with high quality of laser transformation hardening (LTH) can be achieved by choosing the working condition using the developed mathematical models.
3. The laser heat input linearly increases with increasing laser power and decreasing scanning speed.
4. The hardened bead width linearly increases with increasing laser power and decreasing scanning speed. Laser power plays very significant role in the hardened bead dimensions. Decrease in scanning speed and the focused position (i.e. from -10mm to -30mm) the hardened bead width increases.
5. The parameters those significantly affecting the hardened depth are scanning speed and laser power respectively. Hardened depth increases as laser power increases and scanning speed decreases. As scanning speed increases, hardened depth decreases considerably and as focused position increases hardened depth decreases marginally.
6. It is evident that angle of entry of hardened bead profile increases with increase in laser power and decrease in scanning speed. It has been also concluded that angle of entry of hardened bead profile increases with increase in laser power, a decrease in scanning speed and increase in focused position i.e. from -30mm to -10mm.
7. It is evident that the bead geometry provides a useful tool to manipulate the hardened bead width and hardened depth during LTH. It is clearly observed that the hardened width linearly increases defocused beam, i.e. with higher beam spot size. Depth of hardened surface increases linearly with decrease in defocused position from -30mm to -10mm.

ACKNOWLEDGEMENTS

The authors are grateful to the management of the Welding Research Institute (WRI), BHEL, Tiruchirappalli-620014, Tamil Nadu, India for extending the facilities of Laser Materials Processing Laboratory to carry out the research work. The authors also wish to express their sincere thanks for the constant encouragement received from the faculties of MANIT Bhopal during the course of the work.

REFERENCES

1. Badkar DS, Pandey KS, Buvanashekaran G. Effects of Laser Phase Transformation Hardening Parameters on the Heat Input and Hardened-Bead Profile Quality of Commercially pure Titanium. *International Journal of Transactions of Nonferrous Metals Society of China*. 2010; 20(6): 1078–1091p.
2. Reisgen U, Schleser M, Mokrov O, Ahmed E. Optimization of laser welding of DP/TRIP steel sheets using statistical approach. *Optics & Laser Technology*. Feb 2012; 44(1): 255–262P.
3. Pal K, Bhattacharya S, Pal SK. Optimization of weld deposition efficiency in pulsed MIG welding using hybrid neuro-based techniques. *International Journal of Computer Integrated Manufacturing.* 2011; 24(3): 198–210p.
4. Padmanaban G, Balasubramanian V. Optimization of pulsed current gas tungsten arc welding process parameters to attain maximum tensile strength in AZ31B magnesium alloy. *International Journal of Transactions of Nonferrous Metals Society of China*. 2011; 21: 467–476p.
5. Kumar S, Rao PS, Ramakrishna A. Effects of eccentricity and arc rotational speed on weld bead geometry in pulsed GMA welding of 5083 aluminum alloy. *Journal of Mechanical Engineering Research.* Jun 2011; 3(6): 186–196p.
6. Zhang XY, Zhang YS. Optimization for Laser Welding Fillet Joint Based on

Response Surface Method. *Advanced Materials Research.* 2011; 211–212: 1110–1114p.
7. Palanivel R, Mathews PK, Murugan N. Development of mathematical model to predict the mechanical properties of friction stir welded AA6351 aluminum alloy. *Journal of Engineering Science and Technology Review*. 2011; 4(1): 25–31p.
8. Khorram A, Ghoreishi M, Mohammad Yazdi RS, Moradi M. Optimization of Bead Geometry in CO_2 Laser Welding of Ti 6Al 4V Using Response Surface Methodology. 2011; 3(7): 708–712p.
9. Rajakumar S, Muralidharan C, Balasubramanian V. Optimization of the friction-stir-welding process and tool parameters to attain a maximum tensile strength of AA7075–T6 aluminium alloy. Proceedings of the Institution of Mechanical Engineers, Part B: Journal of Engineering Manufacture. 2010; 224(8): 1175–1191p.
10. Vairism, Petousis M. Designing experiments to study welding processes: using the Taguchi method. *Journal of Engineering Science and Technology Review.* 2009; 2(1): 99–103p.
11. Benyounis KY, Olabi AG. Optimization of different welding processes using statistical and numerical approaches-A reference guide. *Journal Advances in Engineering.* 2008; 39(6): 483–496p.
12. Alidoosti A, Ghafari-Nazari1 A, Moztarzadeh F, Jalali N, Moztarzadeh S, Mozafari M. Electrical discharge machining characteristics of nickel–titanium shape memory alloy based on full factorial design. *Journal of Intelligent Material Systems and Structures.* Sep 2013; 24(13): 1546–1556p.
13. Chen SL, Shen D. Optimisation and Quantitative Evaluation of the Qualities for Nd-YAG Laser Transformation Hardening. *The International Journal of Advanced Manufacturing Technology*. Jan 1999; 15(1): 70–78p.
14. Ruifeng Li, Jin Y, Li Z, Qi K. A Comparative Study of High-Power Diode Laser and CO_2 Laser Surface Hardening of AISI 1045 Steel. *Journal of Materials Engineering and Performance.* Sep 2014; 23(9): 3085–3091p.
15. Liu S, Kovacevic R. Statistical analysis and optimization of processing parameters in high-power direct diode laser cladding. *The International Journal of Advanced Manufacturing Technology*. Sep 2014; 74(5–8): 867–878p.
16. Zhao Y, Zhang Y, Hu W, Lai X. Optimization of laser welding thin-gage galvanized steel via response surface methodology. *Optics and Lasers in Engineering.* 2012; 50(9): 1267–1273p.
17. Douglas CM. Statistical Quality Control. 2nd Edn, John Wiley and Sons.
18. Milton JS, Jesse CA. Introduction of Probability and Statistics. 2nd Edn, McGraw-Hill.
19. Stephen RS, Robert GL. Understanding Industrial Designed Experiments. 4th Edn, Air Academy Press.
20. Charles RH. Fundamental Concepts in the Design of Experiments. 4th Edn, Oxford University Press. www.welding-consultant.com.
21. Box GEP, Wilson KB. On the Experimental Attainment of Optimum Conditions," Journal of the Royal Statistical Society, Series B. 1951; 13(1): 1–38p.
22. Montgomery DC. Design and Analysis of Experiments. 2nd Edn, Wiley, New York, 2007.
23. Box GEP, Behnken DW. Some new three level designs for the study of quantitative variables. Technometrics. 2nd Edn 2, 1960; 455–475p.
24. Montgomery, Douglas C. Design and Analysis of Experiments. John Wiley & Sons Inc. 2009.
25. Laser materials processing lab, Welding Research Institute (WRI), Bharat Heavy Electricals Limited (BHEL), 2008–2009, Trichy-620014, Tamil Nadu, India.

Cite this Article
Duradundi Sawant Badkar. Research on Laser Hardened Bead Geometry in Laser Hardening Parameters of ASTM Grade3 Pure Titanium. *Research & Reviews: Journal of Physics.* 2017; 6(1): 22–37p.